

Supporting Information

Ru dopants induced tensile strain in Ni₂P for efficient urea-assisted water decomposition at an ampere-level current density

Mengmeng Wang^{a,b}, Yunmei Du^{a,b,*}, Shuangshuang Li^{a,b}, Yuanxiang Gu^b and Lei Wang^{a,c,*}

^a Key Laboratory of Eco-chemical Engineering, Ministry of Education, International Science and Technology Cooperation Base of Eco-chemical Engineering and Green Manufacturing, Qingdao University of Science and Technology, Qingdao 266042, P. R. China.

^b Shandong Engineering Research Center for Marine Environment Corrosion and Safety Protection, College of Environment and Safety Engineering, Qingdao University of Science and Technology, Qingdao 266042, P. R. China.

^c College of Chemistry and Molecular Engineering, Qingdao University of Science and Technology, Qingdao 266042, China.

*E-mail: duyunmei@qust.edu.cn (Yunmei Du); inorchemwl@126.com (Lei Wang)

Figures and Tables

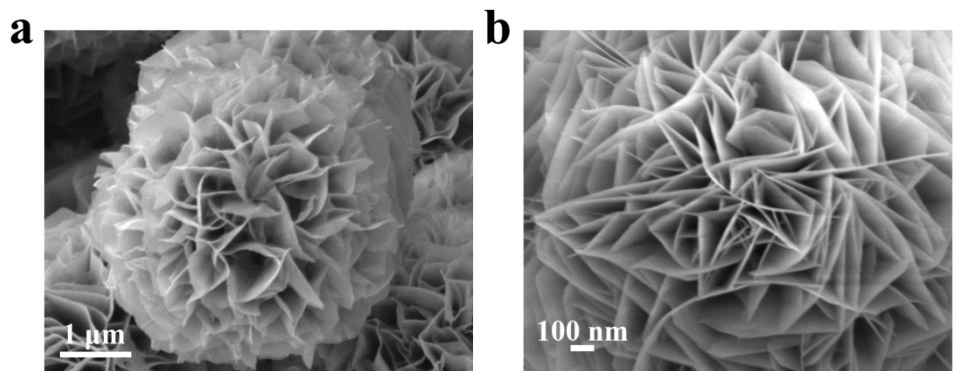


Figure S1. SEM image of N-Ni(OH)₂.

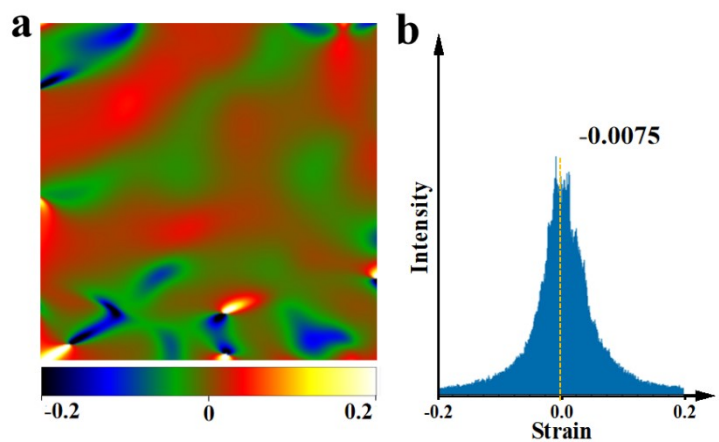


Figure S2. a) The exy strain component using geometric phase analysis (GPA) algorithm, and b) histogram of strain distribution of Ru-Ni₂P@CN.

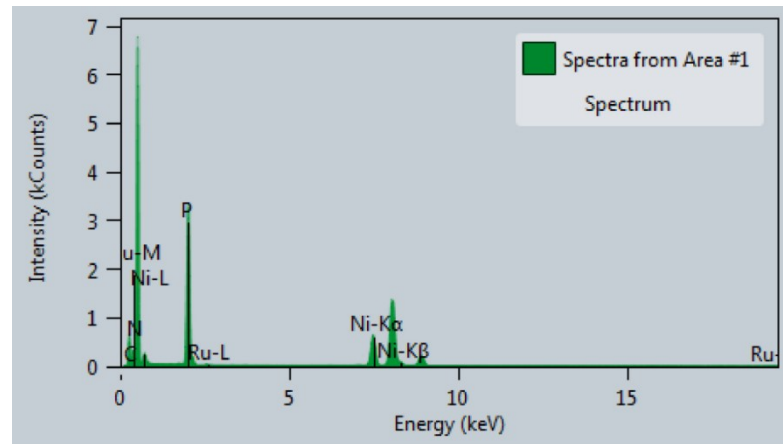


Figure S3. EDX of Ru-Ni₂P@CN catalyst.

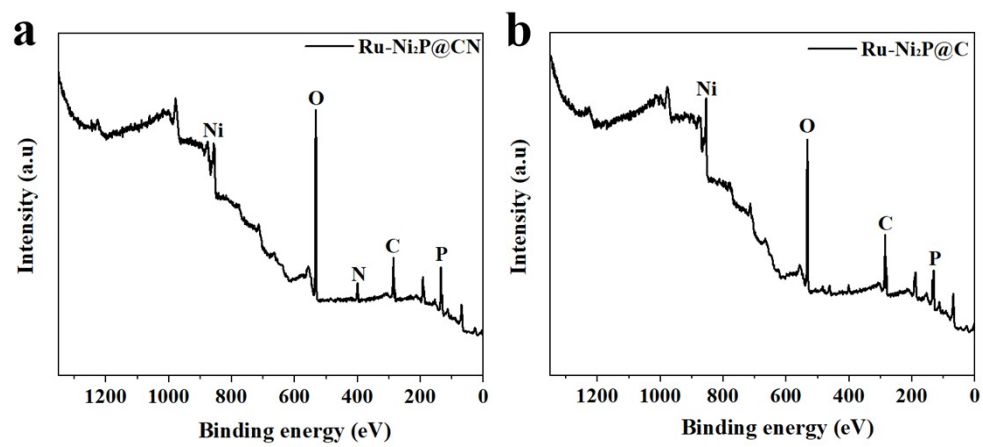


Figure S4. XPS measured the spectra of Ru-Ni₂P@CN and Ru-Ni₂P@C.

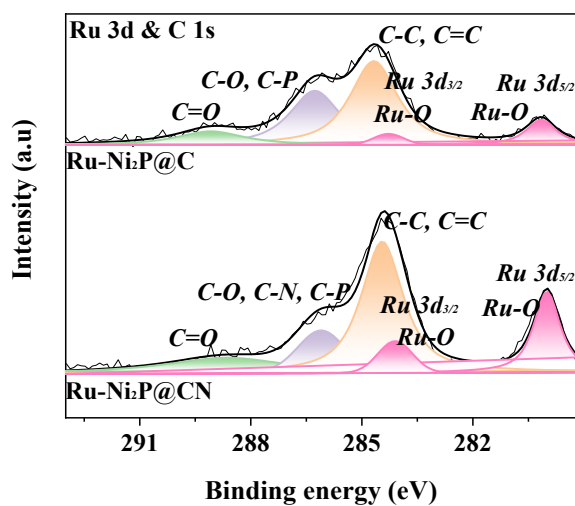


Figure S5. XPS measured the spectra of Ru-Ni₂P@CN and Ru-Ni₂P@C.

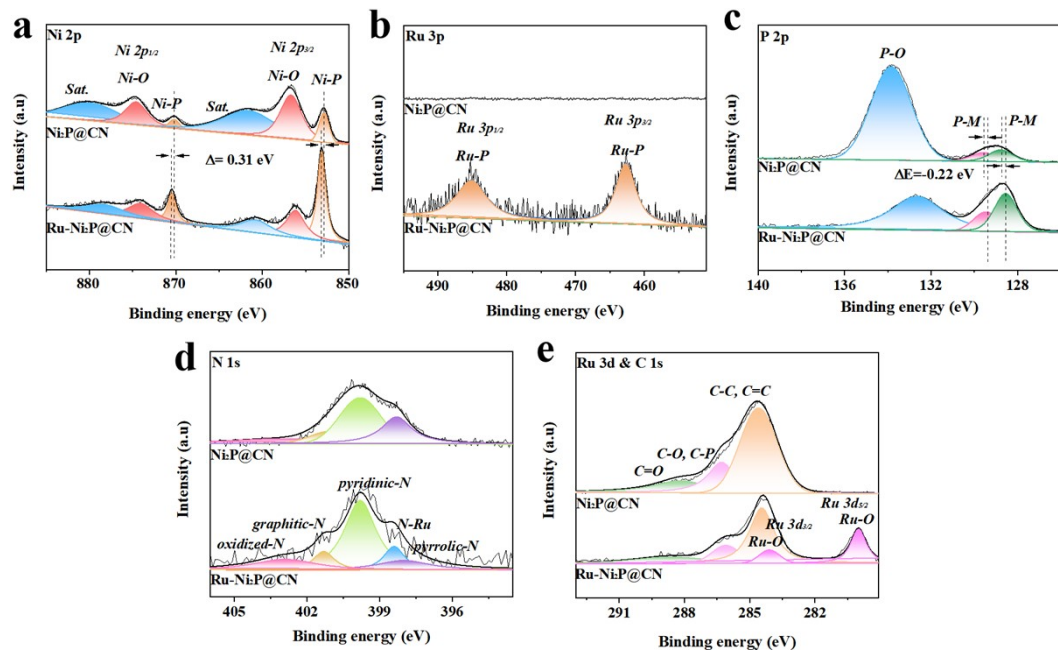


Figure S6. High-resolution spectra of (a) Ni 2p. (b) Ru 3p. (c) P 2p. (d) N 1s. (e) Ru 3d & C 1s.

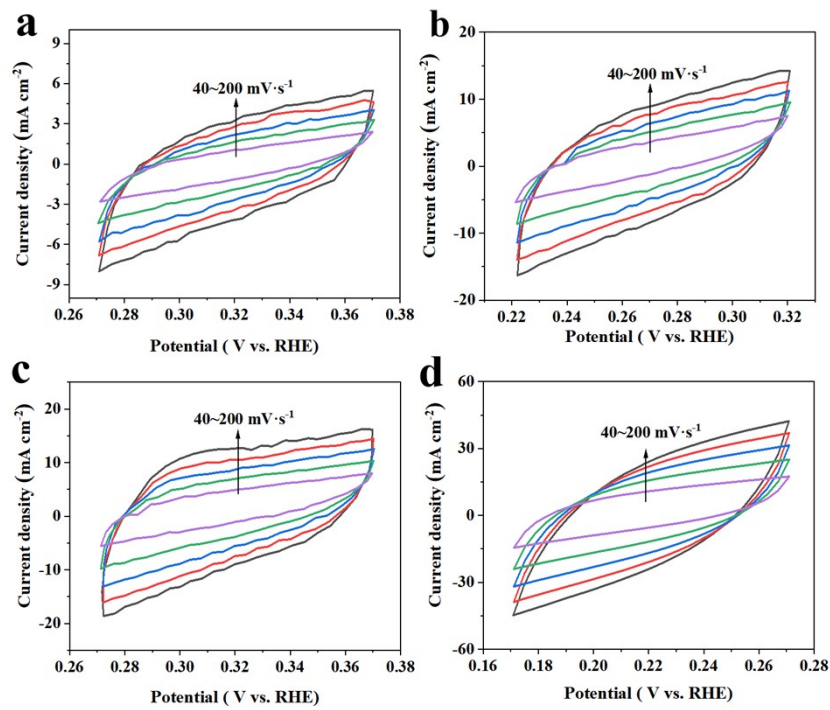


Figure S7. a) CV curves of the non-faradic region for $\text{Ni}_2\text{P}@\text{CN}$, (b) $\text{Ru}-\text{Ni}_2\text{P}$, (c) $\text{Ru}-\text{Ni}_2\text{P}@\text{CN}$ and (d) $\text{Ru}-\text{Ni}_2\text{P}@\text{C}$.

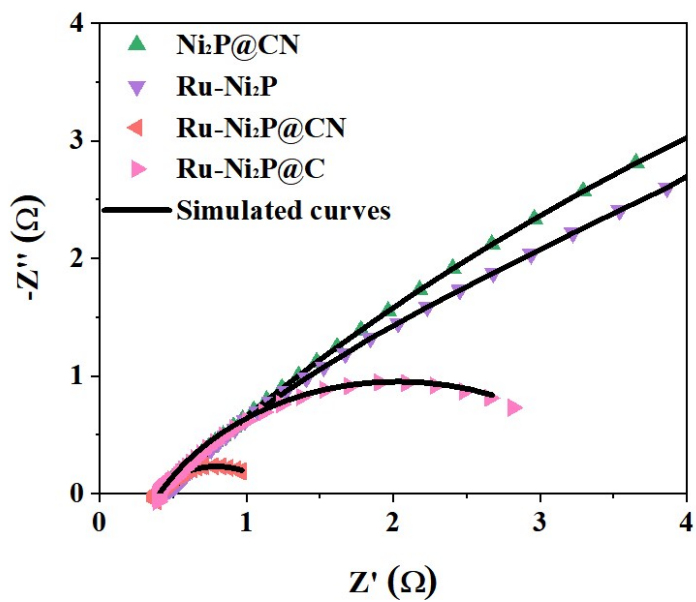


Figure S8. Nyquist and Bode plots for Ni₂P@CN, Ru-Ni₂P, Ru-Ni₂P@CN and Ru-Ni₂P@C in 1.0 M KOH.

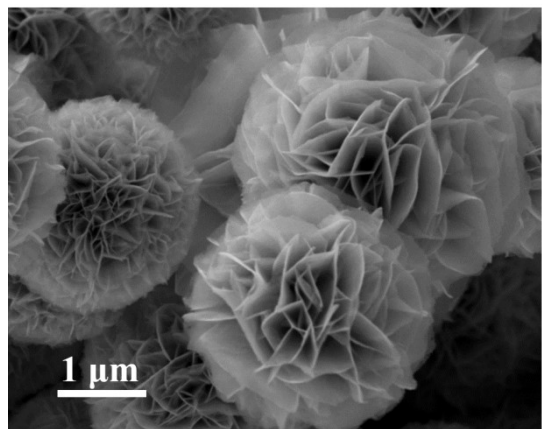


Figure S9. SEM of Ru-Ni₂P@CN after HER.

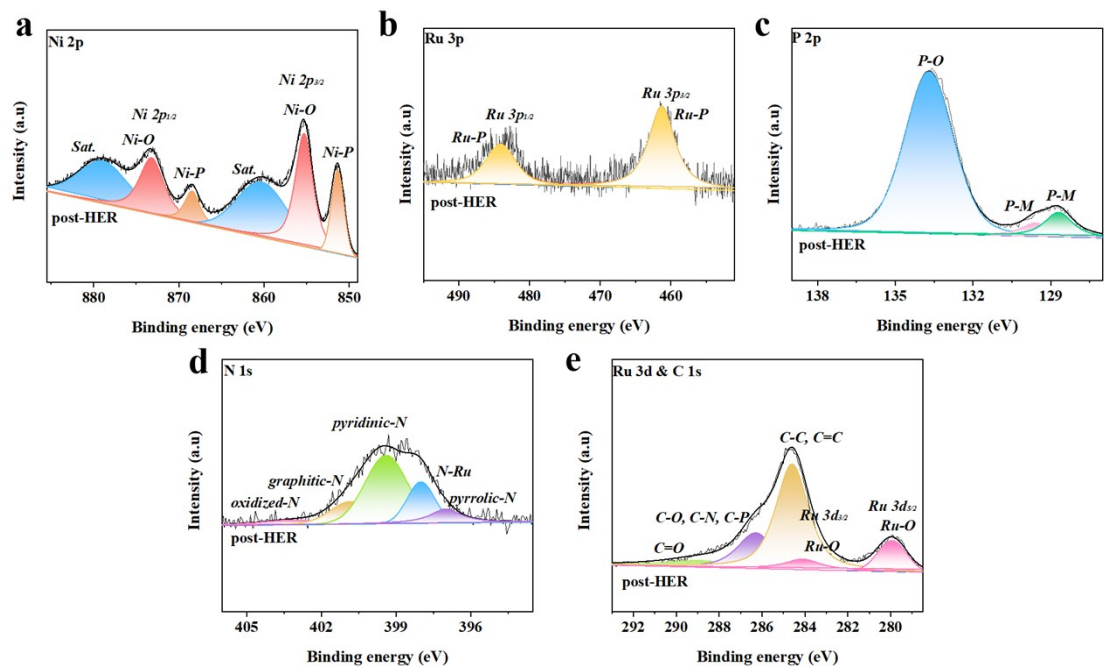


Figure S10. XPS spectra of the Ru-Ni₂P@CN after HER stability test: (a) Ni 2p, (b) Ru 3p, (c) P 2p, (d) N 1s, and (e) Ru 3d & C 1s spectrum.

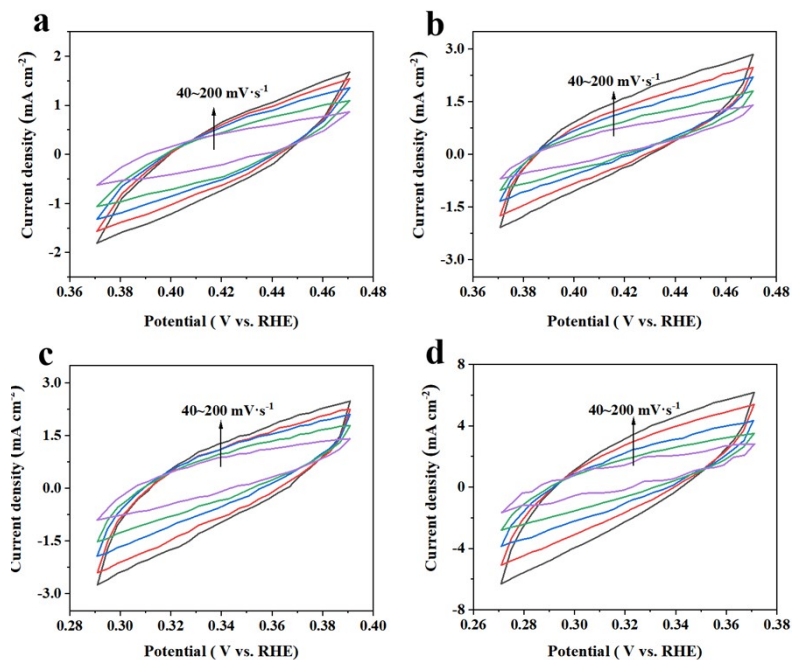


Figure S11. a) CV curves of the non-faradic region for Ni₂P@CN, (b) Ru-Ni₂P, (c) Ru-Ni₂P@CN and (d) Ru-Ni₂P@C

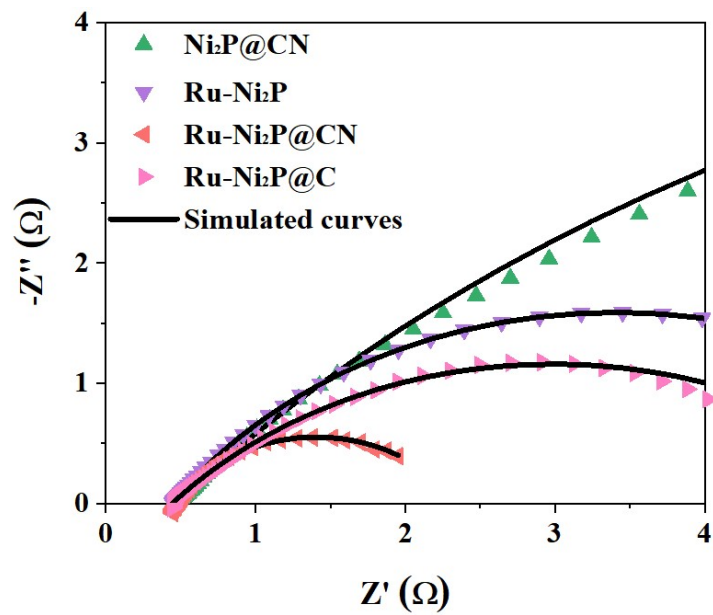


Figure S12. Nyquist and Bode plots for Ni₂P@CN, Ru-Ni₂P, Ru-Ni₂P@CN and Ru-Ni₂P@C in 1.0 M KOH and 0.5 M urea.

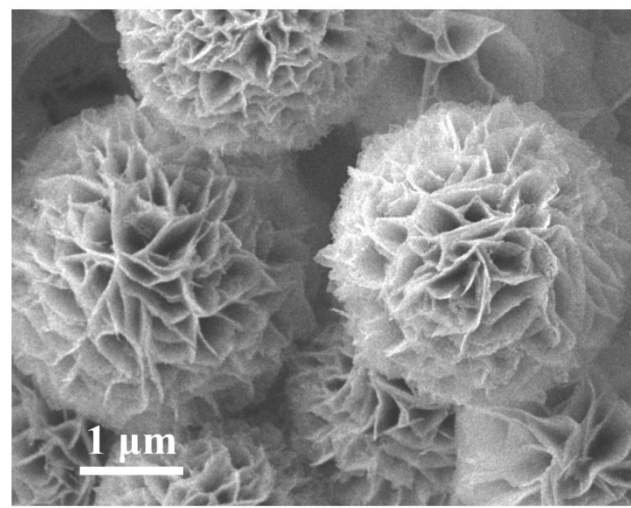


Figure S13. SEM of Ru-Ni₂P@CN after UOR.

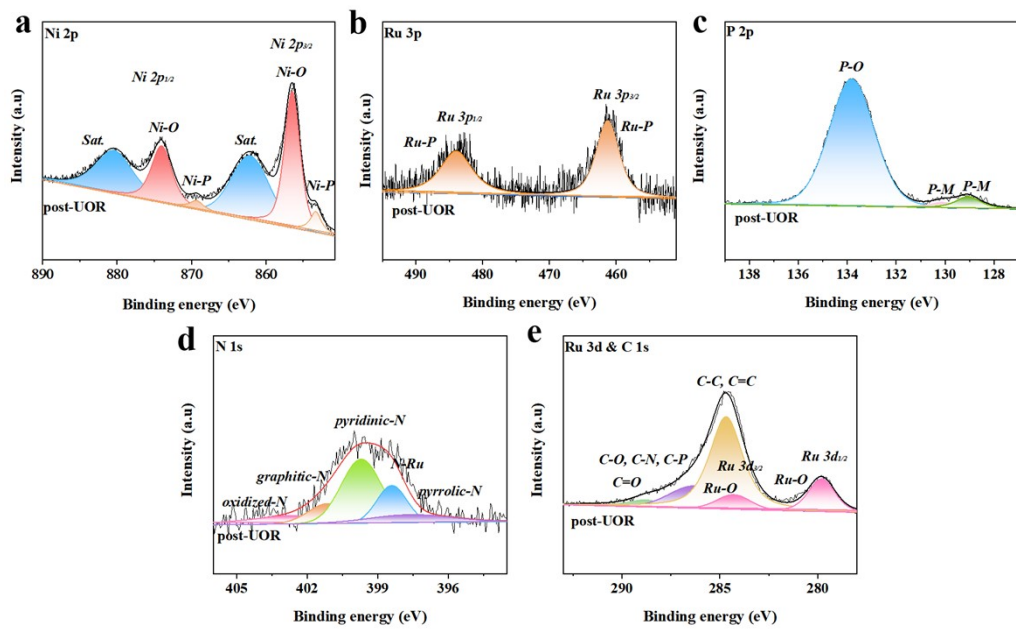


Figure S14. XPS spectra of the Ru-Ni₂P@CN after UOR stability test: (a) Ni 2p, (b) Ru 3p, (c) P 2p, (d) N 1s, and (e) Ru 3d & C 1s spectrum.

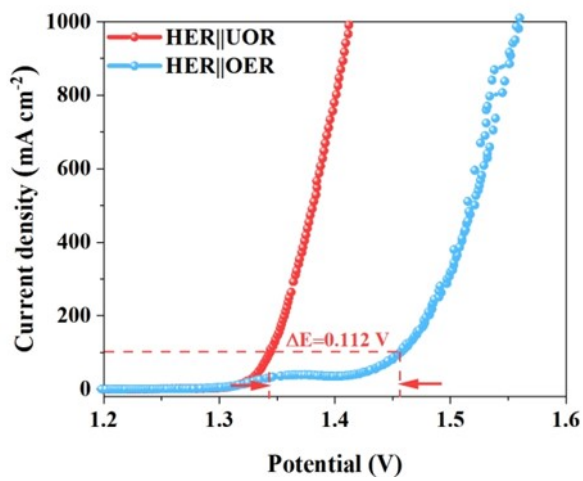


Figure S15. Electrocatalytic overall water splitting performance of Ru-Ni₂P@CN||Ru-Ni₂P@CN in 0.5 M urea solution was compared with that of Ru-Ni₂P@CN||Ru-Ni₂P@CN in 1.0 M KOH.

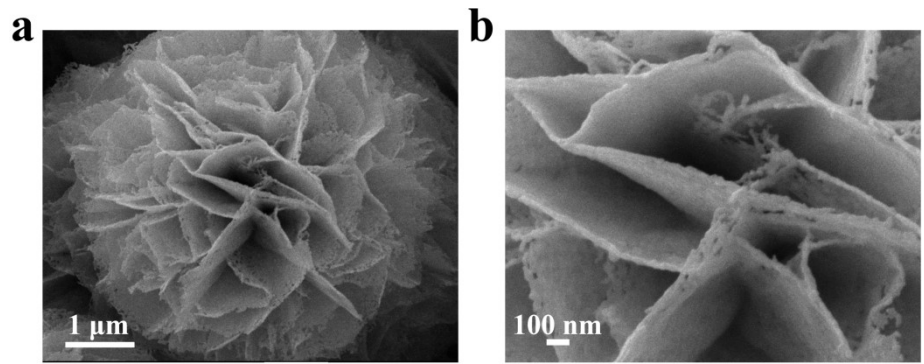


Figure S16. SEM image of Ru-Ni₂P@CN-5.

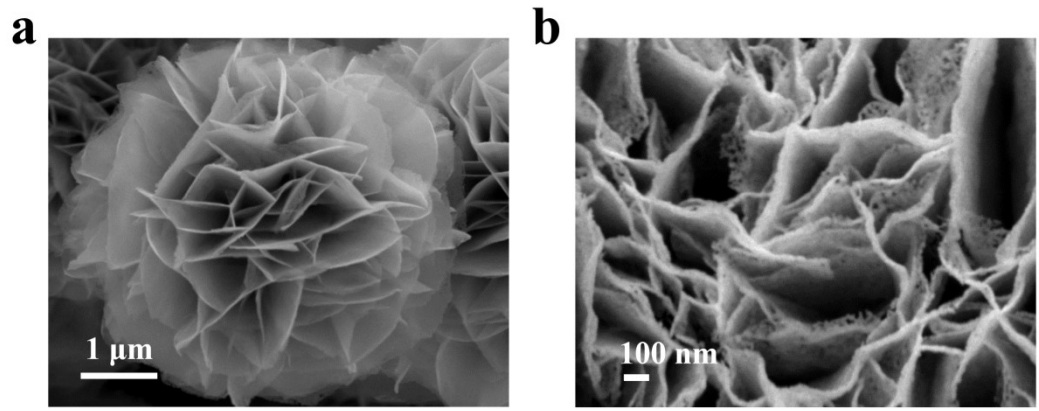


Figure S17. SEM image of Ru-Ni₂P@CN-10.

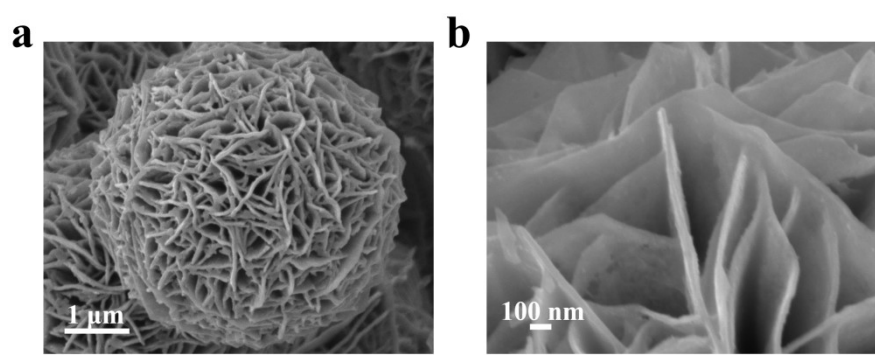


Figure S18. SEM image of Ru-Ni₂P@CN-20.

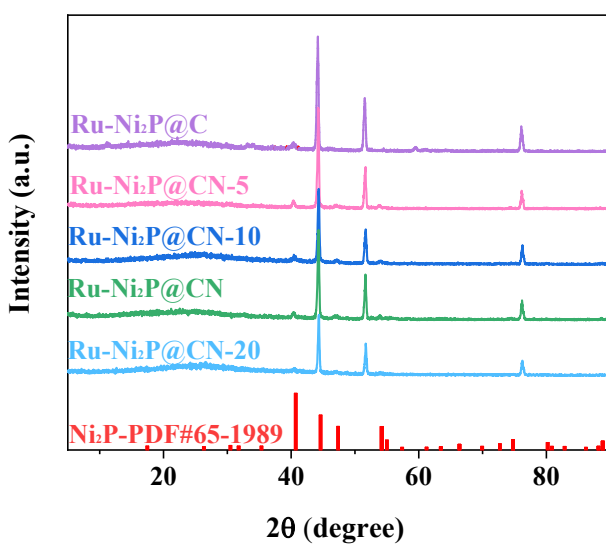


Figure S19. XRD patterns of Ru-Ni₂P@C, Ru-Ni₂P@CN-5, Ru-Ni₂P@C-10, Ru-Ni₂P@C, and Ru-Ni₂P@CN-20.

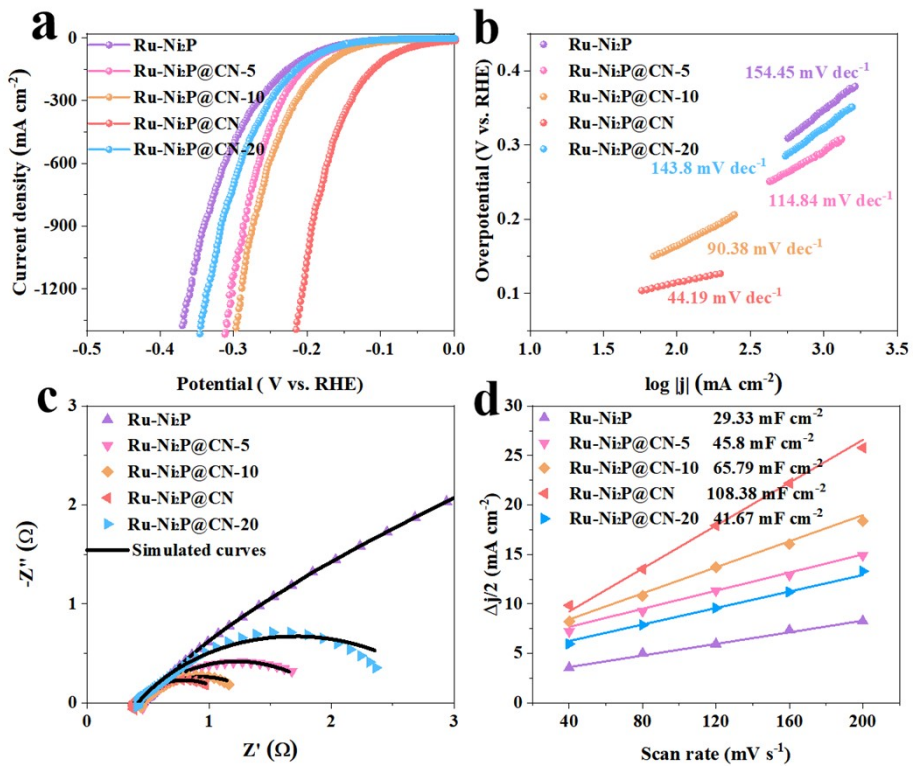


Figure S20. a) LSV curves of Ru-Ni₂P, Ru-Ni₂P@CN-5, Ru-Ni₂P@CN-10, Ru-Ni₂P@CN, and Ru-Ni₂P@CN-20 in 1.0 M KOH. b) Tafel slopes. c) EIS charts d) C_{dl} plots of Ru-Ni₂P@C, Ru-Ni₂P@CN-5, Ru-Ni₂P@CN-10, Ru-Ni₂P@CN, and Ru-Ni₂P@CN-20.

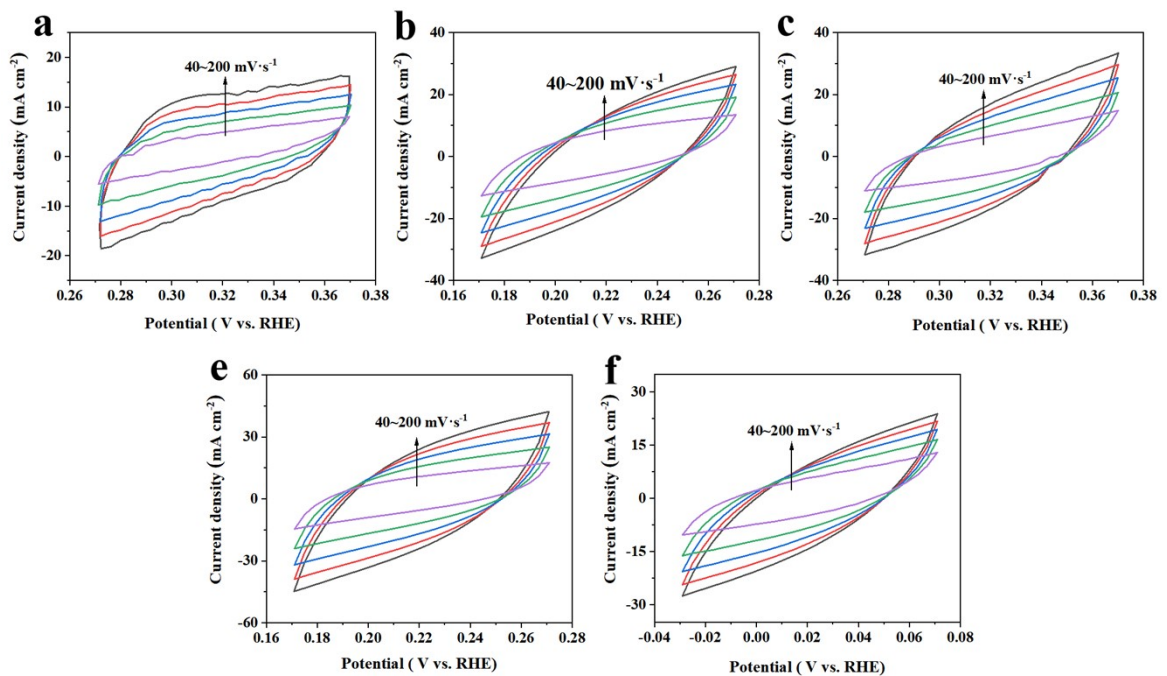


Figure S21. CV curves of the non-faradic region for (a) Ru-Ni₂P@C, (b) Ru-Ni₂P@CN-5, (c) Ru-Ni₂P@CN-10, (d) Ru-Ni₂P@CN, and (d) Ru-Ni₂P@CN-20.

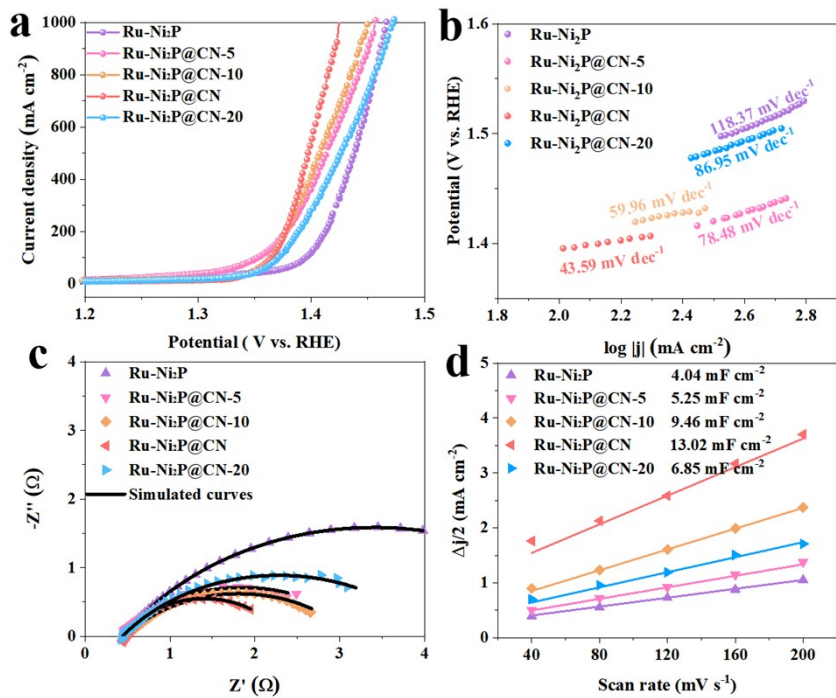


Figure S22. a) LSV curves of Ru-Ni₂P, Ru-Ni₂P@CN-5, Ru-Ni₂P@CN-10, Ru-Ni₂P@CN, and Ru-Ni₂P@CN-20 in 1.0 M KOH. b) Tafel slopes. c) EIS charts d) C_{dl} plots of RuNi₂P@C, Ru-Ni₂P@CN-5, Ru-Ni₂P@CN-10, Ru-Ni₂P@CN, and Ru-Ni₂P@CN-20.

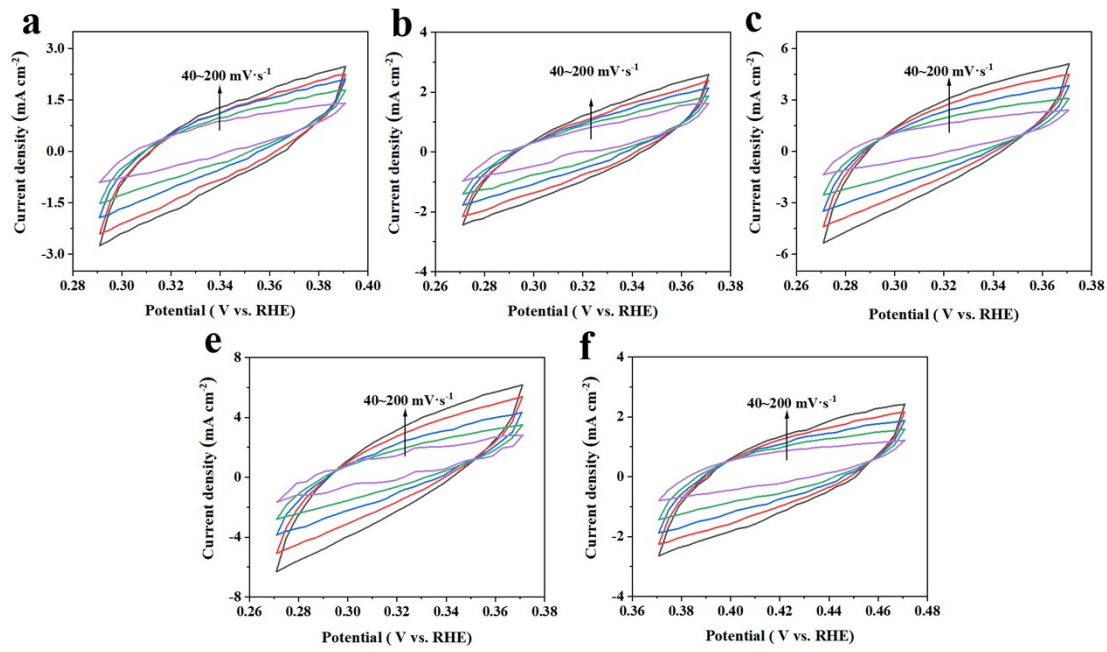


Figure S23. CV curves of the non-faradic region for (a) Ru-Ni₂P@C, (b) Ru-Ni₂P@CN-5, (c) Ru-Ni₂P@CN-10, (d) Ru-Ni₂P@CN, and (d) Ru-Ni₂P@CN-20.

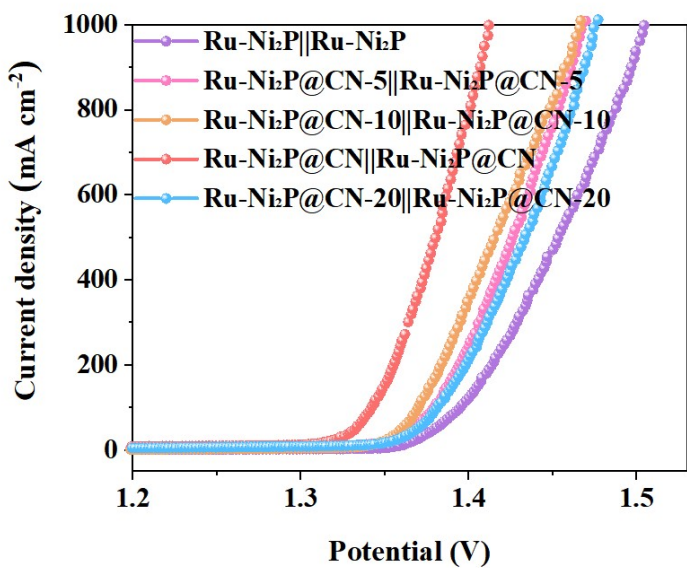


Figure S24. Electrocatalytic overall water splitting performance of Ru-Ni₂P, Ru-Ni₂P@CN-5, Ru-Ni₂P@CN-10, Ru-Ni₂P@CN, and Ru-Ni₂P@CN-20 in 0.5 M urea solution.

Table S1. Comparison of Ru, Ni, P, N, and C contents in different electrocatalysts obtained from XPS tests.

Electrocatalysts/element(at%)	Ru	Ni	P	N	C
Ru-Ni ₂ P@C	0.34	14.55	32.66	0	48.45
Ru-Ni ₂ P@CN	0.69	12.86	29.26	8.12	47.38

Table S2. Comparison of electrochemical surface area (ECSA) of Ru-Ni₂P@CN catalyst and other comparative samples for HER.

Electrocatalysts	C _{dl} (mF cm ⁻²)	C _{DL} (mF)	ECSA (cm ⁻²)
Ni ₂ P@CN	17.9	17.9	447.5
Ru-Ni ₂ P	29.33	29.33	733.25
Ru-Ni ₂ P@CN	108.38	108.38	2709.5
Ru-Ni ₂ P@C	74.28	74.28	1857

C_{DL}=C_{dl}*S; S=1*1 cm²; ECSA=C_{DL}/C_s; C_s=0.04 mF cm⁻².

Table S3. Internal resistance (R_Ω) and charge transfer resistance (R_{ct}) of Ru- $\text{Ni}_2\text{P}@\text{CN}$ catalyst and other comparative samples for HER

Electrocatalysts	$R_\Omega(\Omega)$	$R_{ct}(\Omega)$
$\text{Ni}_2\text{P}@\text{CN}$	0.43	18.16
Ru- Ni_2P	0.46	12.89
Ru- $\text{Ni}_2\text{P}@\text{CN}$	0.40	0.66
Ru- $\text{Ni}_2\text{P}@\text{C}$	0.42	2.93

Table S4. The overpotential required for excessive metal-based electrocatalysts was recently reported in an alkaline environment of 1000 mAc⁻².

Catalyst	HER η_{1000} (mV)	References
this work	255	□
Ni/MoO ₂ @CN	267	[1]
Ni ₂ (1-x)Mo _x P	294	[2]
Ni ₃ P/MnOOH/NF	268	[3]
Ni ₂ P/NF	306	[4]
F, P-Fe ₃ O ₄ /IF	321.3	[5]
NiP ₂ -FeP ₂	327	[6]
Ni ₂ P-Fe ₂ P/NF	333	[7]
FeWO ₄ -Ni ₃ S ₂ @C/NF	343	[8]
A-NiCo LDH/NF	384	[9]
Pt/C/NF	431	[9]
HC-Mo ₂ S/Mo ₂ C	441	[10]
Pd ₄ S/Pd ₃ P _{0.95}	486	[11]

Table S5. ICP results of Ru before and after HER of Ru-Ni₂P@CN

Sample	Ru content (at%)
Initial	0.72
After-HER	0.70

Table S6. Comparison of electrochemical surface area (ECSA) of N-Ru₂P@Ru catalyst and other comparative samples for UOR.

Electrocatalysts	C _{dl} (mF cm ⁻²)	C _{DL} (mF)	ECSA (cm ⁻²)
Ni ₂ P@CN	175.81	175.81	4395.25
Ru-Ni ₂ P	118.37	118.37	2959.25
Ru-Ni ₂ P@CN	43.59	43.59	1089.75
Ru-Ni ₂ P@C	62.77	62.77	1569.25

C_{DL}=C_{dl}*S; S=1*1 cm²; ECSA=C_{DL}/C_s; C_s=0.04 mF cm⁻².

Table S7. Internal resistance (R_Ω) and charge transfer resistance (R_{ct}) of Ru-Ni₂P@CN catalyst and other comparative samples for UOR

Electrocatalysts	$R_\Omega(\Omega)$	$R_{ct}(\Omega)$
Ni ₂ P@CN	0.48	13.48
Ru-Ni ₂ P	0.46	5.58
Ru-Ni ₂ P@CN	0.46	1.76
Ru-Ni ₂ P@C	0.47	4.14

Table S8. The potential required for a noble metal-based electrocatalyst in 0.5 M urea solution environment at 10 mA cm⁻² has recently been reported.

Catalyst	The electrolyte	Potential (V)	References
this work	1 M KOH+0.5M Urea	1.31	□
NiO/Ni ₂ P/NF-40	1 M KOH+0.33 M Urea	1.338	[12]
Co ₂ P/NiMoO ₄	1 M KOH+0.5M Urea	1.34	[13]
Ni-DMAP-2/NF	1 M KOH+0.5 M Urea	1.34	[14]
MOF-Ni@ MOF-Fe-S	1 M KOH+0.33 M Urea	1.347	[15]
Ni ₂ P/MoO ₂ /NF	1 M KOH+0.5 M Urea	1.35	[16]
Fc-NiCo-BDC	1 M KOH+0.33 M Urea	1.35	[17]
P-Mo-Ni(OH) ₂	1.0 M KOH +0.1 M urea	1.35	[18]
NiF ₃ /Ni ₂ P	1 M KOH+0.33 M Urea	1.36	[19]
Ni-MOF	1 M KOH+0.33 M Urea	1.37	[20]
Ni@NCNT	1 M KOH+0.5 M Urea	1.38	[21]
MoP@NiCo-LDH/NF-20	1 M KOH+0.5 M Urea	1.392	[22]
CoO-Co ₄ N@NiFe-LDH	1 M KOH+0.33 M Urea	1.393	[23]

Table S9. The potential required for a noble metal-based electrocatalyst in 0.5 M urea solution at 10 mA cm⁻² has recently been reported.

Catalyst	Pitential (V)	References
this work	1.313	□
Ru-Ni ₃ N@NC	1.36	[24]
Ni(OH)S/NF	1.36	[25]
NiSe ₂ -NiMoO ₄	1.37	[26]
NiS@Ni ₃ S ₂ /NiMoO ₄	1.4	[27]
P-CoNi ₂ S ₄	1.4	[28]
Ni-Mo nanotube	1.43	[29]
NiCo ₂ S ₄	1.45	[30]
Ni-S-Se/NF	1.47	[31]
Ni ₂ P/Fe ₂ P/NF	1.47	[32]
Ni ₂ P/CFC	1.48	[33]
Ni(OH) ₂ -PBA-P	1.5	[34]
NiF ₃ /Ni ₂ P@CC-2	1.54	[35]

Table S10. Internal resistance (R_Ω) and charge transfer resistance (R_{ct}) of Ru- $\text{Ni}_2\text{P}@\text{CN}$ catalyst and other comparative samples for HER

Electrocatalysts	$R_\Omega(\Omega)$	$R_{ct}(\Omega)$
Ru-Ni ₂ P	0.46	12.89
Ru-Ni ₂ P@CN-5	0.46	1.40
Ru-Ni ₂ P@CN-10	0.44	0.82
Ru-Ni ₂ P@CN	0.40	0.66
Ru-Ni ₂ P@CN-20	0.42	2.13

Table S11 Internal resistance (R_Ω) and charge transfer resistance (R_{ct}) of Ru- $\text{Ni}_2\text{P}@\text{CN}$ catalyst and other comparative samples for UOR

Electrocatalysts	$R_\Omega(\Omega)$	$R_{ct}(\Omega)$
Ru-Ni ₂ P	0.46	5.58
Ru-Ni ₂ P@CN-5	0.46	2.58
Ru-Ni ₂ P@CN-10	0.47	2.47
Ru-Ni ₂ P@CN	0.46	1.76
Ru-Ni ₂ P@CN-20	0.48	3.31

References

1. G. F. Qian, J. L. Chen, T. Q. Yu, J. C. Liu, L. Luo and S. B. Yin, *Nano-Micro Lett.*, 2022, **14**, 1-15.
2. F. Yu, H. Q. Zhou, Y. F. Huang, J. Y. Sun, F. Qin, J. M. Bao, W. A. Goddard, S. Chen and Z. F. Ren, *Nat. Commun.*, 2018, **9**, 2551.
3. L. Yu, I. K. Mishra, Y. L. Xie, H. Q. Zhou, J. Y. Sun, J. Q. Zhou, Y. Z. Ni, D. Luo, F. Yu, Y. Yu, S. Chen and Z. F. Ren, *Nano Energy*, 2018, **53**, 492-500.
4. X. Y. Zhang, F. T. Li, R. Y. Fan, J. Zhao, B. Dong, F. L. Wang, H. J. Liu, J. F. Yu, C. G. Liu and Y. M. Chai, *J. Mater. Chem. A*, 2021, **21**, 15836-15845.
5. A. Kumar, V. Q. Bui, J. S. Lee, A. R. Jadhav, Y. Hwang, M. Gyu Kim, Y. Kawazoe, H. Lee, *ACS Energy Lett.* 2021, **6**, 354-363.
6. X. X. Yu, Z. Y. Yu, X. L. Zhang, Y. R. Zheng, Y. Duan, Q. Gao, R. Wu, B. Sun, M. R. Gao, G. X. Wang and S. H. Yu, *J. Am. Chem. Soc.*, 2019, **141**, 7537-7543.
7. H. H. Tang, Y. F. Qi, D. N. Feng, Y. Y. Chen, L. Y. Liu, L. Hao, K. F. Yue, D. S. Li and Y. Y. Wang, *Sustain. Energy Fuels*, 2022, **19**, 4477-4483.
8. Z. L. Wang, G. F. Qian, T. Q. Yu, J. L. Chen, F. Shen, L. Luo, Y. J. Zou and S. B. Yin, *Chem. Eng. J.*, 2022, **434**, 134669.
9. H. Y. Yang, Z. L. Chen, P. F. Guo, B. Fei, R. B. Wu, *Appl. Catal. B Environ.*, 2020, **261**, 118240.
10. C. Zhang, Y. T. Luo, J. Y. Tan, Q. M. Yu, F. N. Yang, Z. Y. Zhang, L. S. Yang, H. M. Cheng and B. L. Liu, *Nat. Commun.*, 2020, **11**, 3724.
11. G. F. Zhang, A. H. Wang, L. W. Niu, W. Gao, W. Hu, Z. H. Liu, R. M. Wang and J. B. Chen, *Adv. Energy Mater.*, 2022, **11**, 2103511.
12. X. Xu, S. J. H. Wang, X. Y. Wang, V. Linkov and R. F. Wang, *J. Colloid Interf. Sci.*, 2022, **615**, 163-172.
13. M. Z. You, S. S. Yi, G. X. Zhang, W. M. Long and D. L. Chen, *J. Colloid Interface Sci.*, 2023, **5**, 184.
14. H. Jiang, S. Y. Bu, Q. L. Gao, J. Long, P. F. Wang, C. S. Lee and W. J. Zhang, *Mater. Today Energy*, 2022, **27**, 101024.

15. H. Z. Xu, K. Ye, K. Zhu, J. L. Yin, J. Yan, G. L. Wang and D. X. Cao, *Dalton Trans.*, 2020, **49**, 5646-5652.
16. X. Xu, S. Ji, H. Wang, X. Y. Wang, V. Linkov and R. F. Wang, *J. Colloid Interf. Sci.*, 2022, **615**, 163-172.
17. M. Li, H. C. Sun, J. M. Yang, M. Humayun, L. F. Li, X. F. Xu, X. Y. Xue, A. Habibi-Yangjeh, K. Temst and C. D. Wang, *Chem. Eng. J.*, 2022, **430**, 132733.
18. W. H. Zhang, Y. H. Tang, L. M. Yu and X. Y. Yu, *Appl. Catal. B Environ.*, 2020, **260**, 118154.
19. K. L. Wang, W. Huang, Q. H. Cao, Y. J. Zhao, X. J. Sun, R. Ding, W. W. Lin, E. H. Liu and P. Gao, *Chem. Eng. J.*, 2022, **427**, 130865.
20. D. D. Zhu, C. X. Guo, J. L. Liu, L. Wang, Y. Du and S. Z. Qiao, *Chem. Commun.*, 2017, **53**, 10906-10909.
21. Q. Zhang, F. MD. Kazim, S. X. Ma, K. G. Qu, M. Li , Y. G. Wang, H. Hu, W. W. Cai and Z. H. Yang, *Appl. Catal. B Environ.*, 2021, **280**, 119436.
22. T. Wang, H. M. Wu, C. Q. Feng, L. Zhang and J. J. Zhang, *J. Mater. Chem. A*, 2020, **8**, 18106-18116.
23. B. J. Chen, M. Humayun, Y. D. Li, H. M. Zhang, H. C. Sun, Y. Wu and C. D. Wang, *ACS Sustain. Chem. Eng.*, 2021, **9**, 14180-14192.
24. Y. B. Liu, D. B. Zheng, Y. Zhao, P. Shen, Y. X. Du, W. P. Xiao, Y. M. Du, Y. L. Fu, Z. X. Wu and L. Wang, *Int. J. Hydrogen Energy*, 2022, **47**, 25081-25089.
25. X. Jia, H. J. Kang, X. X. Yang, Y. L. Li, K. Cui, X. H. Wu, W. Qin and G. Wu, *Appl. Catal. B: Environ.*, 2022, **312**, 121389.
26. T. Q. Yu, Q. L. Xu, J. L. Chen, G. F. Qian, X. Y. Zhuo, H. F. Yang and S. B. Yin, *Chem. Eng. J.*, 2022, **449**, 137791.
27. L. Sha, T. Liu, K. Ye, K. Zhu, J. Yan, J. Yin, G. Wang, D. Cao, *J. Mater.s Chem. A*, 2020, **8**, 18055-18063.
28. X. F. Lu, S. L. Zhang, W. Sim, S. Y. Gao, X. W. David Lou, *Angew. Chem. Int. Ed.*, 2021, **60**, 22885.
29. J. Y. Zhang, T. He, M. D. Wang, R. J. Qi, Y. Yan, Z. H. Dong, H. F. Liu, H. M. Wang and B. Y. Xia, *Nano Energy*, 2019, **60**, 894-902.

30. J. Wang, Y. Sun, Y. F. Qi and C. Wang, *ACS Appl. Mater. Interfaces*, 2021, **13**, 57392-57402.
31. N. Chen, Y. X. Du, G. Zhang, W. T. Lu and F. F. Cao, *Nano Energy*, 2021, **81**, 105605.
32. L. Yan, Y. L. Sun, E. L. Hu, J. Q. Ning, Y. J. Zhong, Z. Y. Zhang and Y. Hu, *J. Colloid Interface Sci.*, 2019, **541**: 279-286.
33. X. Zhang, M. M. Han, G. Q. Liu, G. Z. Wang, Y. X. Zhang, H. M. Zhang and H. J. Zhao, *Appl. Catal. B: Environ.*, 2019, **244** , 899-908.
34. H. Z. Xu, K. Ye, K. Zhu, Y. Y. Gao, J. L. Yin, J. Yan, G. L. Wang, D. X. Cao, *ACS Sustain. Chem. Eng.*, 2020, **8**, 16037.
35. K. L. Wang, W. Huang, Q. H. Cao, Y. J. Zhao, X. J. Sun, R. Ding, W. W. Lin, E. H. Liu and P. Gao, *Chem. Eng. J.*, 2022, **427**, 130865.